Electronic structure of Fe/semiconductor/Fe(001) tunnel junctions

M. Freyss,* N. Papanikolaou,† V. Bellini,‡ R. Zeller, and P. H. Dederichs
Institut für Festkörperforschung, Forschungszentrum Jülich, D-52425 Jülich, Germany
(Received 15 February 2002; published 24 July 2002)

The electronic ground-state properties of Fe/semiconductor/Fe(001) tunnel junctions are studied by means of the *ab initio* screened Korringa-Kohn-Rostoker method. We focus on the magnetic properties, charge transfer, local, and $\mathbf{q}_\parallel$-resolved density of states of these systems. We consider in detail Fe/ZnSe/Fe(001) tunnel junctions and compare their electronic properties with junctions with Si and GaAs barriers. We discuss the results in connection to the spin-dependent transport properties expected for these systems.

DOI: 10.1103/PhysRevB.66.014445 PACS number(s): 75.70.Cn, 73.40.Sx, 73.40.Gk

I. INTRODUCTION

Magnetic tunnel junctions are widely studied for their spin-dependent transport properties. They consist of two ferromagnetic metallic films (or leads) separated by a layer of an insulating or semiconducting material. Depending on the relative orientation of the magnetizations of the two metallic leads, the electrical resistance through the junction can vary substantially. This phenomenon is the so-called tunnel magnetoresistance (TMR). The resistance ratio can vary up to 40% at room temperature with an Al_2O_3 barrier.[1–3] These tunnel junctions are currently investigated for their potential technological applications as nonvolatile magnetic random access memories (MRAM's). The research to find tunnel junctions with large TMR ratios requires the understanding of the underlying physical phenomenon. Little is still known about the relationship between the electronic band structure of the tunnel junctions and the resulting TMR values. It has, however, been observed that the electronic structure of the metal/barrier interface plays a fundamental role in the transport properties.[4] Furthermore the Jullière model,[5] which accounts for the TMR in terms of the properties of the magnetic leads only, namely, the spin polarization of the bulk density of state at the Fermi level, is not valid for such junctions. An accurate calculation of the interface electronic properties, possibly by an *ab initio* approach, is thus very desirable.

An *ab initio* study for the electronic structure of some Fe/semiconductor/Fe junctions was already reported by Butler *et al.*[6,7] using the layered Korringa-Kohn-Rostoker (KKR) method. Moreover the same group have used the Landauer formula to calculate the TMR on Fe/ZnSe/Fe junctions. These calculations show that in epitaxial systems the tunneling strongly depends on the $\mathbf{q}_\parallel$ value and the symmetry of the incident Blochwave of the ferromagnet. For sufficiently thick barriers only the states of perpendicular incidence can penetrate the semiconductor, leading to TMR values of close to 100%. The same group[8] as well as Mathon *et al.*[9] have also reported calculations for Fe/MgO/Fe(001). Among other features these calculations show that interface states in the minority band can strongly influence the tunneling magnetoresistance for intermediate thicknesses. Independently, Oleinik *et al.*[10] have calculated the electronic and structural properties of $Co/Al_2O_3/Co$ tunnel junctions by approximating the amorphous alumina barrier by a crystalline phase.

In this paper, we focus on semiconductor tunnel barriers, in particular ZnSe, but also GaAs and Si. Contrary to the commonly used Al_2O_3 insulating barrier, semiconductors such as ZnSe, GaAs, and Si grow epitaxially in the zinc blende structure on bcc Fe. This is possible due to the small lattice mismatch between Fe and ZnSe, GaAs, and Si (5.4, 1.6, and 1.3 %, respectively). Furthermore, ZnSe can be grown on Fe at room temperature without interdiffusion.[11] Experiments also suggests that Se and As are surfactant to Fe.[11,12] In our theoretical study, we concentrate in particular on the electronic structure of the interface and extend previous calculations of Butler *et al.*[6,7] by considering the effect of the different terminations of the interface. We find that both the terminations as well as the geometrical structure of the interface influence strongly the magnetic properties. In addition we discuss the role of metal induced gap states as well as resonant interface states for the tunneling and magnetoresistance.

The article is organized as follows. In the next section, we present the *ab initio* screened KKR method used to obtain the ground-state properties of the tunnel junctions. In Sec. III, the results are discussed: the magnetic properties, the charge transfer at the interface, the local density of states (LDOS), the $\mathbf{q}_\parallel$-resolved density of states ($\mathbf{q}_\parallel$-DOS), and finally the spin polarization in the leads and the barrier.

II. THEORETICAL METHOD

The electronic structure was calculated using the screened Korringa-Kohn-Rostoker Green's function method. A central concept in the KKR Green's function method is the use of the Dyson equation

$$\mathbf{G} = \mathbf{G}^r + \mathbf{G}^r \Delta V \mathbf{G} \tag{1}$$

to connect the Green's functions of the true physical system $\mathbf{G}$ with an arbitrarily chosen reference system described by $\mathbf{G}^r$. Here $\mathbf{\Delta} V = V - V^r$ is the difference of the corresponding potentials. The idea of the screened KKR (SKKR) method is the construction of a reference system for which the Green's function decays exponentially in real space. This would lead to short ranged interactions limited to neighboring atoms only. For this purpose we use a lattice of constant and strongly repulsive muffin-tin potentials. In that way we can

accomplish screening and thus a tight-binding-like, nearly band-diagonal form for the structural Green's function matrix of this reference system. The true physical system is not required to have short range interactions. The KKR and SKKR methods and their properties are described in details elsewhere.[13–15] Here we will briefly discuss the application of the SKKR to layered structures and semi-infinite systems.

The Dyson equation (1) can be transformed in an algebraic matrix form by using the usual site-angular momentum expansion.[14] For layered systems with 2D periodicity we use a 2D Fourier transform. Due to the exponential decay of the screened structure constants, the coupling can be limited to few neighboring shells, so that the 2D Fourier transform of the reference Green's function has the structure of a band matrix coupling only neighboring layers. By using the concept of principal layers,[16,17] the problem reduces to a Dyson equation for a linear chain with nearest neighbor coupling only.

For such systems, the diagonal blocks of the real system Green's function can be calculated with a computational effort that scales linearly with the number N of principal layers in the slab, as was shown by Godfrin[18] and Wu *et al.*[19] Only these blocks are required in order to obtain the charge density $n(\mathbf{r};E)=-(1/\pi)\mathrm{Im}\,G(\mathbf{r},\mathbf{r};E)$. This N-scaling behavior is one of the main advantages of the screened KKR approach.

The band diagonal form of the Green's function allows us to treat semi-infinite systems also. For this we can divide the system in three regions: an intermediate region (I), embedded into two (unperturbed) semi-infinite left (L) and right (R) half spaces. The regions R and L are characterized by bulk potentials, so that the self-consistency process affects only the potentials in region I. Using an inversion-by-partitioning technique it is easy to see that embedding region I into the semi-infinite L and R host media only affects the top-left G^{11} and bottom-right G^{NN} principal layer blocks of the Green's function matrix. This embedding information is included in the surface Green's function G^{11}_{surf} (left half space), G^{NN}_{surf} (right half space) which we obtain by using an iterative procedure, the so-called decimation method as described in Refs. 16,20. Usually 5–6 decimation steps are sufficient to obtain well converged surface Green's functions. Only a few $\mathbf{q}_{\parallel}$ points (e.g., close to van Hove singularities) require additional effort. The calculation for the embedded system, i.e., the evaluation of the site-diagonal Green's function in region I, scales linearly with the number N of principal layers in the region I.

For the calculations in this study, we assume spherical ASA (atomic sphere approximation) potentials and a cutoff of the wave functions at $l_{\max}=3$, while the full charge density is included. The open structure of the semiconductor zinc blende lattice and the assumption of ASA potentials require the introduction of an empty sphere in each (001) atomic plane. Moreover we use the local density approximation of density functional theory in the parametrization of Vosko *et al.*[21]

III. RESULTS: ELECTRONIC GROUND-STATE PROPERTIES

In our KKR calculations, the tunnel junctions are modeled by two semi-infinite bcc Fe(001) half crystals separated by a semiconducting film of ZnSe, GaAs, or Si. We assume a perfect matching of the bcc lattice of Fe with the zinc blende lattice of the semiconductors, so that no lattice relaxations are allowed and all atoms are fixed at the positions as determined by the lattice constant of Fe. We take the experimental value of the Fe lattice constant of a=10.85 a.u. (if not indicated otherwise). For this structure the zinc blende lattice constant is double as large as the bcc constant of Fe, so that each Fe layer contains two non-equivalent Fe atoms. The potentials of the semiconductor layers as well as the potentials of four Fe layers on both sides of the junction are calculated self-consistently, while all other Fe potentials are replaced by their bulk values. For the zinc blende semiconductors ZnSe (or GaAs) the (001) film consists of a stacking of Zn and Se layers, so that two interfaces with Fe have to be distinguished: a Zn-terminated Fe/ZnSeZn$\cdots$ interface or a Se-terminated Fe/SeZnSe$\cdots$ interface. As we will show in the following, the electronic properties of the junction depend sensitively on the termination.

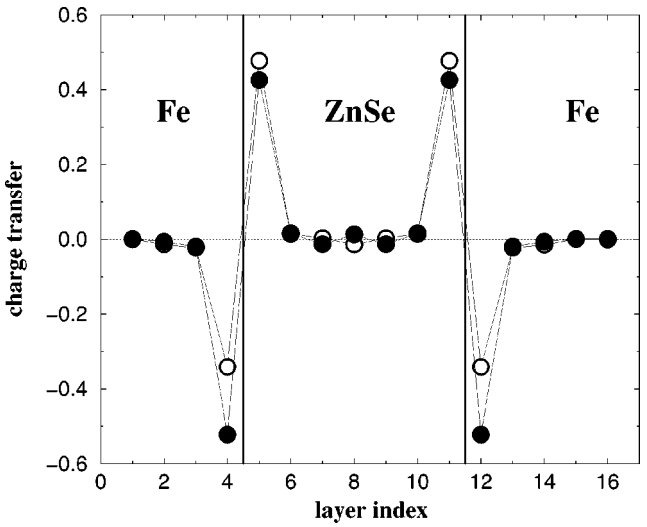

FIG. 1. Charge transfer per atomic layer in an Fe/7 ZnSe/Fe(001) junction with Zn termination (full circles) and Se termination (open circles). Note that the charge transfer is defined with respect to the charge of the bulk layer of Fe and the Zn and Se layers in bulk ZnSe.

A. Charge transfer

The charge transfer is shown in Fig. 1 for both Zn- and Se-terminated Fe/7-ML ZnSe/Fe(001) junctions. The figure represents the charge transfer per atomic layer in each layer relative with respect to the bulk charges, which are 30.22 for Zn layers, 33.78 for Se layers and two times 26.00 for Fe layers. A large charge transfer occurs at the interface: electrons are transferred from Fe to the semiconductor. This charge transfer is found to be very localized. It is mostly limited to the last Fe and to the first semiconductor atomic layers at the interface. With Zn at the interface, around 0.52 electrons are missing at the Fe layer, i.e., 0.26 electrons per Fe atoms, and are mostly transferred to the neighboring Zn layer. In the junctions with the other barriers considered, the charge transfer follows a similar trend. In the Se-terminated

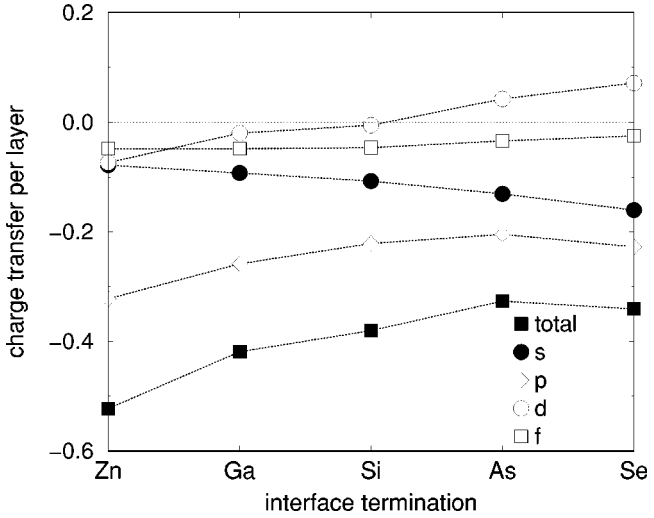

FIG. 2. *l*-decomposed charge transfer of an interfacial Fe atom for junctions with different barriers and terminations. The dotted lines are guides to the eyes.

Fe/ZnSe/Fe(001) junctions, the charge transferred from Fe amounts to 0.34 electrons per layer (see Fig. 1, open symbols). In Fe/Si/Fe, it is 0.38 electrons, and in Fe/GaAs/Fe, it is 0.42 for the Ga termination and 0.33 for the As termination.

Our results are somewhat different from the results obtained by Butler *et al.* In their study of Zn-terminated Fe/ZnSe/Fe(001) (Ref. 6) and Ga-terminated Fe/GaAs/Fe(001) (Ref. 7) junctions, the charge transfer is less localized. While the charge transfer for the two interface layers is similar to ours, in addition a sizable and opposite charge transfer of almost 0.2 electrons is obtained for the second Fe and the second semiconductor layer. Note that in the semiconductors slab, our definition of the charge transfer refers to the bulk charges, so that the perturbation with respect to the bulk is visible also in the middle of the barrier. On the contrary the plots in the works of MacLaren *et al.*[6] and Butler *et al.*[7] refer to the charges of the neutral layers. For comparison the charge transfer of the bulk must be added for ZnSe and GaAs while Si has neutral layers and our results can be compared directly. The present results are, however, in agreement with recent TB-LMTO calculations for Fe/Si/Fe(001) by Turek *et al.*,[22] who obtain an equally localized charge transfer of the same size as we do.

Since the *sp* elements Zn, Ga, Si, As, and Se have a larger electronegativity than Fe, one intuitively expects that the charge flows from Fe to the *sp* elements. Using the same argument, one would also expect the largest charge transfer to occur for a Se-terminated ZnSe film (Fig. 1), since Se has the largest electronegativity. In fact, the largest charge transfer occurs for the termination with Zn, having the smallest electronegativity of the elements considered. Thus the behavior is more complicated. This shows up also in Fig. 2 where the change of the charge of the interfacial Fe layer is decomposed, for the ZnSe, GaAs, and Si systems, into *s*, *p*, *d*, and *f* contributions and plotted against the valence of the terminating layer. One finds a loss of *s* charge increasing with the valence of the *sp* elements, a large loss of *p* charge, slightly

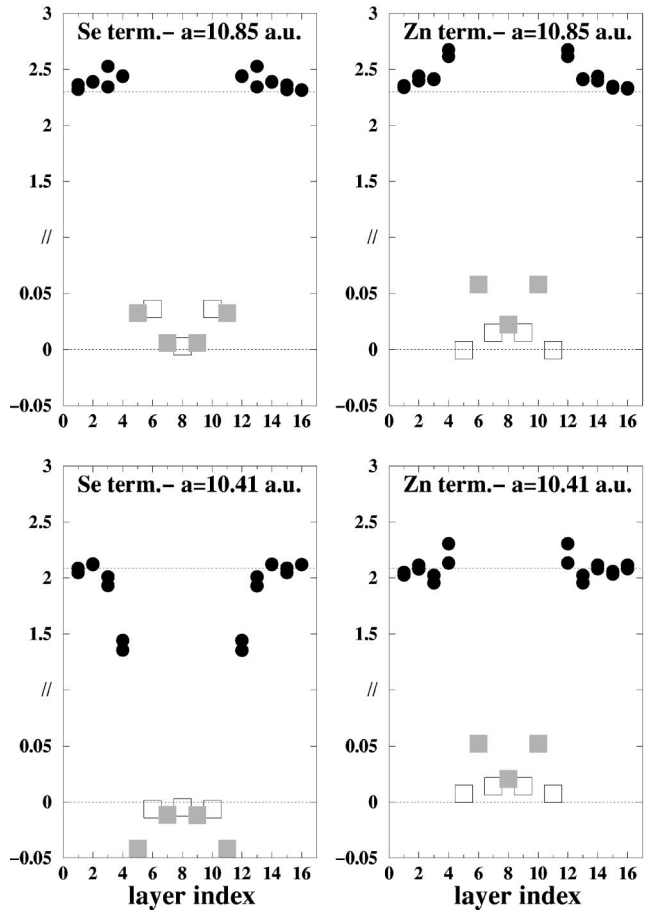

FIG. 3. Magnetic profile in Fe/7 ZnSe/Fe(001) junction with Zn termination and Se termination, and with the experimental (above) and ''theoretical'' lattice constant (below) as obtained in LDA calculation. Full circles are for Fe, squares for Zn (open symbols) and Se (full symbols). Note that for the small induced moments in the semiconductor layers the scale has been enlarged by a factor of 10.

decreasing with the valence, a gain of *d* charge, at least for the higher valent elements and a small slightly decreasing loss of *f* charge. Some of us have found the same trend, some years ago, in calculations for *sp* impurities in bulk Fe.[23] Here the charge of the Fe neighbors of the impurities shows a strong gain of *d* charge increasing linearly with the valence of the impurity, a loss of *s* charge, also scaling linearly with the valence, and a loss of *p* charge, initially decreasing and then increasing with the valence. The linear scaling of the loss of *s* charge reflects a linear scaling of the isomer shift of the nearest neighbor Fe atoms, which has been found in many Mössbauer experiments.[24] Therefore our calculations for the junctions directly predict for the Fe interface layer an isomer shift of about 0.19 mms^{-1} for a Zn termination and a double as large shift for the Se termination (0.38 $\mathrm{mm\,s}^{-1}$). Thus a measurement of the Fe isomer shift would allow us to determine the termination.

B. Magnetic properties

The magnetization profile for a Fe/ZnSe/Fe(001) junction is shown in Fig. 3, both for the Se and the Zn termination.

Very small moments are induced in the semiconductor layers adjacent to the interface, which are somewhat larger and alternating in the case of the Zn termination. For the Se termination the Fe moments at the interface are practically the same as in the bulk, while for the Zn termination, the interfacial moments are enhanced by $0.34\mu_B$. In both cases, the magnetic moments are only perturbed in 3–4 layers adjacent to the interface, before recovering to the bulk value.

Unfortunately, these results, obtained with the experimental lattice constant of Fe (10.85 a.u.), depend strongly on the choice of the lattice parameter. For the ''theoretical'' value (10.41 a.u.), obtained within the LDA from the minimum of the total energy, the magnetic moments are appreciably reduced. While the bulk moments of Fe change moderately from $2.30\mu_B$ to $2.09\mu_B$, the interface moments are reduced from $2.64\mu_B$ to $2.22\mu_B$ for the Zn termination, and $2.44\mu_B$ to $1.40\mu_B$ for the Se termination. Thus the moment at the interface do not only depend on the termination, but also on the lattice parameter used in the calculations.

Similar effects are also found for a Si barrier, for which the interfacial Fe moments are $2.34\mu_B$ for the experimental and $1.51\mu_B$ for the LDA lattice constant. For the GaAs barrier, we obtain for the Ga termination moments of $2.47\mu_B$ for the experimental and $1.87\mu_B$ for the ''theoretical'' lattice constants, while for the As termination the values are $2.33\mu_B$ and $1.47\mu_B$.

The reduction of the Fe moments due to hybridization with *sp* elements is known from the behavior of dilute ferromagnetic alloys. Basically due to the hybridization of the impurity *p* states with the iron *d* states, *p-d* bonding hydrides of mostly Fe *d* character are formed which strongly affects the occupancy of the Fe majority and minority state. Both *d* states are pushed to lower energies, some *d* intensity is transfered to empty antibonding hybrides above E_F, and the local *d* bands are broadened, leading to unoccupied majority states above E_F. As a result, the Fe moment decreases strongly, and the Fe *d* charge increases weakly as is shown in Fig. 2.

The decrease of the magnetic moments at the interface is related to a decrease in the DOS at E_F in the minority band and an increase in the majority band. As will be shown in the following section, the minority states of Fe at the interface display a strong peak at E_F for the experimental lattice constant. With the reduced LDA lattice parameter, this peak is slightly shifted below E_F. The shift is more pronounced for the As and Se terminations, which results in a larger decrease in the moments than with Ga and Zn terminations.

The magnetic properties are thus very sensitive to the termination of the interface and to the crystal structure. Therefore the relaxation of the interface distances, not taken into account here, or structural defects might have an important effect on the magnetic properties of the system. A detailed study of these effects would require an improved exchange correlation functional such as the generalized gradient approximation (GGA),[25] which gives excellent results for the moment and lattice constant of Fe. This is, however, beyond the scope of this paper.

C. Electronic structure: LDOS and $q_\parallel$-resolved DOS

An important aspect of the electronic structure of the tunnel junctions is the presence of metal-induced gap states (MIGS) in the semiconductor. The existence of such states at metal/semiconductor interfaces has been discussed for a long time[26] but their fundamental role in the spin-dependent transport properties through tunnel junctions was only pointed out recently.[27] MIGS are states from the metal or from the interface with energies in the gap of the semiconductor so that they decay exponentially in the barrier. We compare here the features of such MIGS in junctions with different semiconducting barriers. A special emphasis is put on ZnSe barriers with the two possible terminations since similar conclusions can be drawn for GaAs.

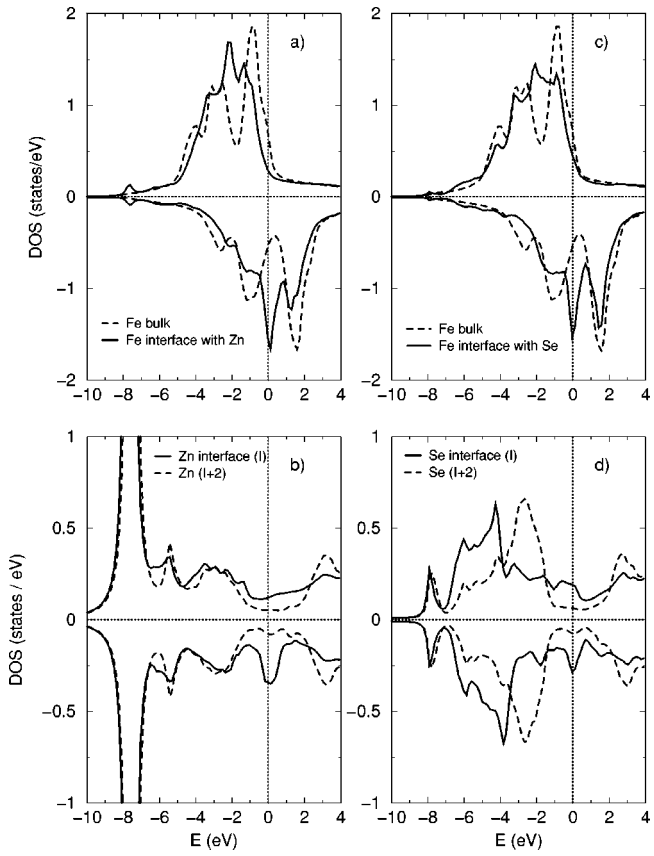

FIG. 4. Density of states (DOS) in an Fe/7 ZnSe/Fe(001) junction with Zn [(a) and (b) left] and Se terminations [(c) and (d), right]. Upper panel: Fe bulk (dashed line) and interface Fe (solid line). Lower panel: semiconductor interface layer (solid line) and two layers away from the interface (dashed line). The vertical dotted line corresponds to the Fermi level.

1. ZnSe barrier with Zn termination

The local density of states (LDOS) in the Zn terminated junction is shown in Figs. 4(a) and 4(b). Figure 4(a) gives the LDOS of bulk Fe (dashed line) and of Fe at the Fe/Zn interface in the junction (solid line). The lower panel [Fig. 4(b)] gives the LDOS of Zn at the interface and of Zn two atomic layers away from the interface. Fe at the interface displays a sharp peak at the Fermi level in the minority band. This state is the analog to the well known Fe(001) surface state[28] and has been observed at different interfaces, and in particular in all the junctions we have studied here with the ZnSe, GaAs,

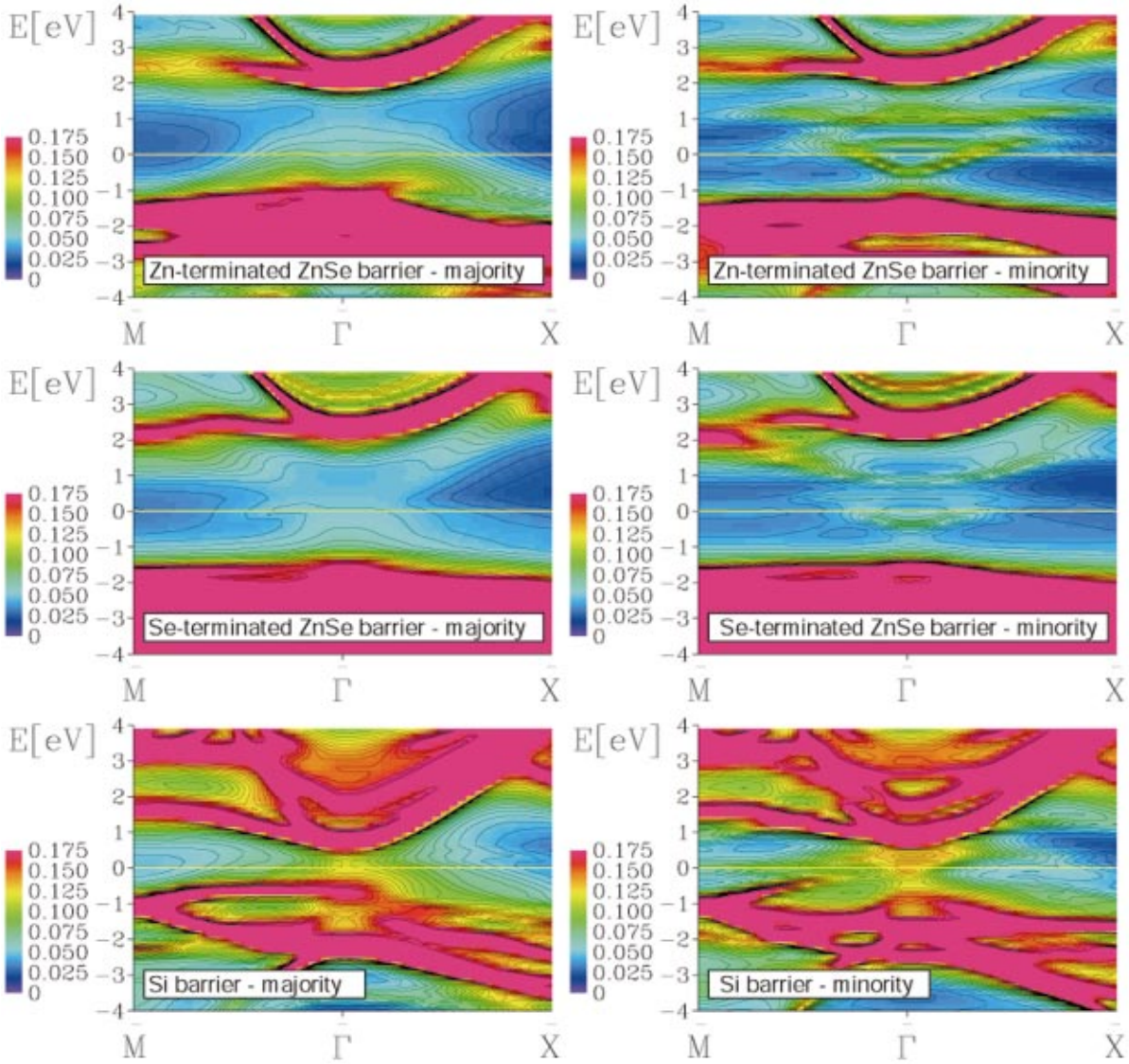

FIG. 5. (Color) $\mathbf{q}_{\|}$-DOS along high symmetry lines of the 2D BZ for the center layer of the semiconducting barrier for energies close to E_F (gap region), in different junctions: Se and Zn terminated Fe/7-ML ZnSe/Fe(001) and Fe/8-ML Si/Fe(001). The yellow line corresponds to the Fermi level. The color scale denotes the number of states [from blue (no states) to red (maximum number of states)]. The lines are contours of equal density.

and Si barriers. It basically consists of dangling *d* bonds of the Fe interface layer, which do not find adequate partners for bonding in the semiconductor. In the majority band the analogous interface state occurs at 2 eV below the Fermi level. In addition, we observe in both bands a considerable band narrowing due to the reduced number of Fe neighbors. In the majority band this leads to a filling of the majority states and thus to an increase of the interface moment above the bulk value (strong ferromagnetism).

The interface state of Fe at E_F in the minority band hybridize weakly with *sp* states in the barrier, to form metal-induced gap states (MIGS), as can be seen from the LDOS of Zn in the minority band [Fig. 4(b)]. These MIGS decrease exponentially in the barrier and already almost vanish in the middle of the 7 ML barrier. States in the gap of ZnSe are also present in the majority band, but with much less intensity than in the minority band. The Fermi level is located at the MIGS peak of the minority band. This pinning of E_F by the MIGS was explained by Tersoff[29] in terms of the charge neutrality at the interface. One also sees in Fig. 4(b) that the thickness of the ZnSe barrier is too small to enable the total decay of the MIGS: in the middle of the barrier, the gap of the semiconductor is still not recovered. However, calculations for larger thicknesses, e.g., 25 ML ZnSe, show that (i) the gap appears with increasing thickness and that (ii) the potentials in the middle of the 7 ML slab are already reasonably well converged to the bulk values. Thus the states in the gap region in Figs. 4(b) and 4(d) are indeed MIGS, which have not yet sufficiently decreased.

The MIGS can be traced up in the two-dimensional Brillouin zone (BZ), as presented in Fig. 5. For each junction considered, the contour plots of the $\mathbf{q}_{\|}$-resolved DOS are

shown along the $\overline{\Gamma}$-$\overline{X}$ and the $\overline{\Gamma}$-$\overline{M}$ directions for the central layer of the barrier, and for both majority (left panels) and minority (right panels) bands. The yellow line indicates the position of the Fermi level, and thus the region of the gap of the semiconductor. The regions of low density of states are expressed by the color *blue* and those of maximum density of states are in *red*. The case of the Zn-terminated junction is shown in the upper panel of Fig. 5. One clearly sees in the minority band the MIGS at E_F which are located around the $\overline{\Gamma}$ point. These states are decaying Fe interface states: they can be found at the same place of the 2D BZ in the $\mathbf{q}_\parallel$-DOS of the Fe interface layer. In the Zn $\mathbf{q}_\parallel$-DOS of the majority band, on the other hand, no such sharp features can be seen at E_F: only very few states remain at E_F around the $\overline{\Gamma}$ point, with much less intensity than in the minority band.

2. ZnSe barrier with Se termination

We consider now the electronic structure of a Fe/ZnSe/Fe(001) barrier with the same 7 ML thickness of ZnSe but with a Se termination. The LDOS in this system is shown on the right panels of Fig. 4: on the top, Fe bulk and interface Fe [Fig. 4(c)], and in the bottom, Se at the interface and Se two monolayers away from the interface [Fig. 4(d)]. One sees again the sharp interface states of Fe in the minority band which can be found decreasing in the semiconductor. Contrary to the Zn-terminated junction, pronounced MIGS are also present in the majority band of Se. This can be related to a local broadening of the *d* band due to the strong hybridization with the Se atoms, leading to empty majority *d* states above the Fermi level signalizing the transition to the weak ferromagnetism of bulk Fe. This shift increases the Fe DOS at E_F in the majority band and partly explains the smaller Fe magnetic moments found at the interface for the Se termination.

Figure 5 shows the $\mathbf{q}_\parallel$ DOS in the middle of the Se-terminated barrier. The picture is relatively similar to the one with a Zn termination. In the minority band, the sharpest features at E_F are located between the $\overline{\Gamma}$ and the $\overline{M}$ points. But only states with weak intensity remain around the $\overline{\Gamma}$ point, in contrast to the Zn terminated junctions. In the majority band, the MIGS present at the interface layer for the Fermi energy [see Fig. 4(d)] have decayed out, and the $\mathbf{q}_\parallel$ DOS presents an analogous feature as for the Zn-terminated interface.

3. Junctions with GaAs and Si barriers

The junctions with a GaAs barrier present several common features with those of a ZnSe barrier. The presence of MIGS in both bands or with more intensity in one band only according to the termination is also found with a GaAs barrier: MIGS in the minority band coming from Fe interface states are present for both terminations but MIGS in the majority band have more intensity for the most electronegative termination As (similar to the case with Se). In the middle of the barrier with Ga termination, weak features at E_F are found in the majority band, whereas in the minority band, there are MIGS for several $\mathbf{q}_\parallel$ values: around the $\overline{\Gamma}$ point, between $\overline{\Gamma}$ and $\overline{M}$ as well as between $\overline{\Gamma}$ and $\overline{X}$. With the As termination, in analogy to the Se termination of the ZnSe barrier, MIGS exists in both bands around the $\overline{\Gamma}$ point.

For the Si barrier, strong features at E_F exist both in the minority and the majority bands, as can be seen on Fig. 5 (lower panels). The gap of Si being smaller than the one of ZnSe and GaAs, the MIGS decrease here slower in the barrier. The MIGS are located at the $\overline{\Gamma}$ point in both majority and minority bands.

TABLE I. Spin polarization $P(E_F)$ in percent at the interface Fe layer and the first semiconductor layer.

		SP (%)
Fe/7 ZnSe (Zn term.)/Fe(001)	Fe	−68
	Zn	−48
Fe/7 ZnSe (Se term.)/Fe(001)	Fe	−54
	Se	−20
Fe/5 GaAs (Ga term.)/Fe(001)	Fe	−59
	Ga	−35
Fe/5 GaAs (As term.)/Fe(001)	Fe	−53
	As	−16
Fe/8 Si/Fe(001)	Fe	−54
	Si	−25

4. Spin-polarization of the MIGS

As it was discussed previously, MIGS show a different behavior in the majority and the minority bands of the semiconductors. A way to quantify the asymmetry between the MIGS of the majority and the minority bands is to calculate the spin polarization P of the density of states at the Fermi energy of the interface layers. The spin polarization P is defined as the following ratio:

$$P = \frac{N^{\uparrow}(E_F) - N^{\downarrow}(E_F)}{N^{\uparrow}(E_F) + N^{\downarrow}(E_F)}, \tag{2}$$

where $N^{\uparrow}(E_F)$ and $N^{\downarrow}(E_F)$ are the density of states at the Fermi energy for the spin-up and spin-down bands, respectively. The spin polarization is calculated for the Fe layer at the interface, as well as for the semiconductor layer at the interface. The P values are listed in Table I.

Interfacial Fe has a large negative polarization due to the sharp interface state at E_F in the minority band. This spin polarization changes slightly according to the barrier or to the termination of the semiconductor film. The values of P for Fe at the interface for the different junctions are −68, −54 % for the ZnSe barrier with a Zn and a Se termination, respectively, −59, −53 % for the GaAs barrier with a Ga and a As termination, and −54% for the Si barrier. Again, we find very similar behavior for the Zn and Ga terminated junction, as well as for the Se and As ones. The reduction of P of about 20 and 10 % for the Se and As termination, respectively, arises partly from the decrease of the minority DOS at E_F and partly from the increase of the majority DOS. This can be seen in Fig. 4 for the Se terminated interface, and is a

consequence of the increased hybridization with the Fe *d* states. Thus the largest polarization is obtained for the most weakly hybridizing Zn termination.

In the semiconducting barrier, the spin polarization of the MIGS is linked to the spin polarization of the current. Thus from an important spin polarization of the MIGS a significant TMR ratio can be expected. Table I gives the spin polarization at E_F in the first semiconductor layer at the interface for the different junctions considered. We see that the spin polarization of the MIGS actually follows the trend of the spin polarization of interface Fe: the biggest value for *P* is obtained for the Zn terminated ZnSe barrier and amounts to almost 50%. For ZnSe and GaAs barriers, the spin polarization decreases by a factor of more than 2 when the most electronegative elements (Se and As) are at the interface. The smallest value for *P* is found for the As terminated GaAs barrier.

IV. SUMMARY

We have presented ground-state calculations for the properties of Fe/semiconductor/Fe(001) junctions with epitaxial interlayers of ZnSe, GaAs, and Si. The calculations use the local density approximation and the screened KKR Green's function method for layered systems. At the interface we find a charge transfer from Fe to the semiconductor, which is strongly localized to the last Fe and the first semiconductor layer and decrease with increasing valence of the *sp* elements at the interface. The Fe moments at the interface depend sensitively on the lattice parameter used in the calculation. For the experimental lattice constant of Fe we find an enhancement of the Fe moments, being largest for the low valent *sp*-interface layer Zn and Ga. On the other hand, for the smaller LDA lattice constant, the Fe moments are strongly decreased, especially for the Se and As interface terminations. Therefore the lattice relaxations at the interface, not included in the present calculations, are expected to play an important role for the electronic and magnetic properties. Finally we have discussed the local density of states and the $\mathbf{q}_\parallel$-resolved density of states at the interface in the energy region of the gap. To a large extent, both are characterized by Fe interface states in the minority band, the $\overline{\Gamma}$ contributions of which extend far into the semiconductor. Explicit calculations of the conductance through Fe/semiconductor/Fe(001) junctions and of the TMR ratio will be presented in a future article.

ACKNOWLEDGMENTS

This work was supported by the TMR-Network Interface Magnetism (Contract No. ERBFMRXCT 960089) and the RT Network Computational Magnetoelectronics (Contract No. RTN1-1999-00145) of the European Commission. We thank Ilja Turek for fruitful discussions and a comparison with his TB-LMTO results for the Fe/Si/Fe(001) junctions.

*Present address: CEA, Direction de l'Energie Nucléaire, Département d'Etudes des Combustibles, Service d'Etudes et de Simulation du Comportement des Combustibles, Centre d'Etudes de Cadarache, 13108 Saint-Paul lez Durance, France.

†Present address: Martin-Luther-Universität, Halle-Wittenberg, Fachbereich Physik, Fachgruppe Theoretische Physik, D-06099 Halle, Germany.

‡Present address: INFM and Dipartimento di Fisica Universitá degli Studi di Modena e Reggio Emilia, Via Campi 213/A, 41100 Modena, Italy.

[1] J. S. Moodera, L. R. Kinder, T. M. Wong, and R. Meservey, Phys. Rev. Lett. **74**, 3273 (1995).

[2] H. Kikuchi, M. Sato, and K. Kobayashi, J. Appl. Phys. **87**, 6055 (2000).

[3] C. Tiusan, T. Dimopoulos, K. Ounadjela, M. Hehn, H. A. M. van den Berg, V. da Costa, and Y. Henry, Phys. Rev. B **61**, 580 (2000).

[4] J. M. De Teresa, A. Barthélémy, A. Fert, J. P. Contour, R. Lyonnet, F. Montaigne, P. Seneor, and A. Vaurès, Phys. Rev. Lett. **82**, 4288 (1999).

[5] M. Jullière, Phys. Lett. **54A**, 225 (1975).

[6] J. M. MacLaren, X.-G. Zhang, W. H. Butler, and X. Wang, Phys. Rev. B **59**, 5470 (1999).

[7] W. H. Butler, X.-G. Zhang, X. Wang, J. van Ek, and J. M. MacLaren, J. Appl. Phys. **81**, 5518 (1997).

[8] W. H. Butler, X.-G. Zhang, T. C. Schulthess, and J. M. MacLaren, Phys. Rev. B **63**, 054416 (2001).

[9] J. Mathon and A. Umerski, Phys. Rev. B **63**, 220403 (2001).

[10] I. I. Oleinik, E. Yu. Tsymbal, and D. G. Pettifor, Phys. Rev. B **62**, 3952 (2000).

[11] E. Reiger, E. Reinwald, G. Garreau, M. Ernst, M. Zölfl, F. Bensch, S. Bauer, H. Preis, and G. Bayreuther, J. Appl. Phys. **87**, 5923 (2000).

[12] Y. B. Xu, E. T. M. Kernohan, D. J. Freeland, A. Ercole, M. Tselepi, and J. A. C. Bland, Phys. Rev. B **58**, 890 (1998).

[13] See, e.g. *Application of Multiple Scattering Theory to Materials Science*, edited by W. H. Butler, P. H. Dederichs, A. Gonis, and R. L. Waever, MRS Symposia Proceedings No. 253 (Materials Research Society, Pittsburgh, 1991).

[14] K. Wildberger, R. Zeller, and P. H. Dederichs Phys. Rev. B **55**, 10 074 (1997).

[15] R. Podloucky, R. Zeller, and P. H. Dederichs, Phys. Rev. B **22**, 5777 (1980); P. J. Braspenning, R. Zeller, A. Lodder, and P. H. Dederichs, *ibid.* **29**, 703 (1984); R. Zeller, J. Phys. C **20**, 2347 (1987).

[16] F. Garcia-Moliner and V. R. Velasco, Prog. Surf. Sci. **21**, 93 (1986).

[17] L. Szunyogh, B. Ujfalussy, P. Weinberger, and J. Kollar, Phys. Rev. **49**, 2721 (1994).

[18] E. M. Godfrin, J. Phys.: Condens. Matter **3**, 7843 (1991).

[19] S. Y. Wu, Z. L. Xie, and N. Potoczak, Phys. Rev. B **48**, 14 826 (1993).

[20] K. Wildberger, Ph.D. thesis, RWTH, Aachen, 1997.

[21] H. Vosko, L. Wilk, and M. Nusair, Can. J. Phys. **58**, 1200 (1980).

[22] I. Turek (private communication).

[23] H. Akai, S. Blügel, R. Zeller, and P. H. Dederichs, Phys. Rev. Lett. **56**, 2407 (1986).

[24] I. Vincze and I. A. Campbell, J. Phys. F: Met. Phys. **3**, 647 (1973).

[25] D. J. Singh, W. E. Pickett, and H. Krakauer, Phys. Rev. B **43**, 11 628 (1991).
[26] V. Heine, Phys. Rev. A **138**, 1689 (1965).
[27] Ph. Mavropoulos, N. Papanikolaou, P. H. Dederichs, and R. Zeller, Phys. Rev. Lett. **85**, 1088 (2000).
[28] N. Papanikolaou, B. Nonas, S. Heinze, R. Zeller, and P. H. Dederichs Phys. Rev. B **62**, 11 118 (2000).
[29] J. Tersoff, Phys. Rev. Lett. **52**, 465 (1984).